

Ground state of liquid helium in the Kirkwood superposition approximation*

M. D. Miller[†]

*Department of Physics and Astronomy, University of Maryland, College Park, Maryland 20742
and Department of Physics and Astronomy, University of Florida, Gainesville, Florida 32611*

(Received 12 May 1976)

We calculate the ground-state energies and pressures for ⁴He and (normal) ³He using radial distribution functions which are solutions of the Born-Bogoliubov-Green-Kirkwood-Yvon (BBGKY) integral equation with the Kirkwood superposition approximation (KSA) used for the three-particle distribution function. We compare the BBGKY-KSA results with those obtained from the hypernetted chain equation, molecular dynamics, and experiment. We conclude that the BBGKY-KSA yields poor results for ⁴He but at the lower ³He densities offers a reasonable approximation to the molecular-dynamics results. The ³He energies are obtained by means of the statistical cluster expansion of Wu and Feenberg and we discuss the convergence of the series. Further, we show that the familiar parametrized power-law form used for the pair function yields pressures consistent with the virial theorem.

I. INTRODUCTION

In the variational approach to the problem of calculating the ground-state energy of an interacting boson system a useful approximation to the N -body wave function is the product of pair functions:

$$\psi_B \equiv \prod_{j>i=1}^N \exp\left[\frac{1}{2}u(r_{ij})\right]. \quad (1.1)$$

In Refs. 1-6 we cite some representative articles from the extensive literature pertaining to the use of ψ_B in the ⁴He problem. The articles basically fall into two categories: those which introduce an explicit parametric form for $u(r)$,¹⁻³ and those which seek to determine $u(r)$ as the solution of an Euler-Lagrange equation.⁴⁻⁶ The evident attraction for the form ψ_B lies in the formal correspondence between the distribution functions which are generated by ψ_B and the distribution functions in the canonical ensemble of classical statistical mechanics. That is, those techniques originally developed for the solution of the classical physics problem can be borrowed for application to the quantum-mechanical problem. In particular, the probabilistic Monte Carlo and molecular-dynamics methods and the solution of approximate integral equations have found the greatest utility.

If one multiplies ψ_B into a Slater determinant of plane waves and spin functions, one obtains an overall antisymmetric function suitable for a variational description of the (normal) ground state of a strongly interacting fermion system. We define this function ψ_F by

$$\begin{aligned} \psi_F &= \prod_{j>i=1}^N \exp\left[\frac{1}{2}u(r_{ij})\right] \mathcal{G}\left(\prod_{i=1}^N e^{i\vec{k}_i \cdot \vec{r}_i} \xi_i(m_i)\right) \\ &= \psi_B \mathcal{G}\left(\prod_{i=1}^N e^{i\vec{k}_i \cdot \vec{r}_i} \xi_i(m_i)\right), \end{aligned} \quad (1.2)$$

where \mathcal{G} is the antisymmetrizer and ξ_i are spin functions. ψ_F is expected to be an adequate description of ³He for temperatures above the superfluid transition (~ 2 mK) but considerably smaller than the Fermi energy (~ 5 °K). Feenberg⁷ has estimated that the quasiparticle picture of Landau for ³He is only valid at temperatures less than ~ 70 mK.

The expectation value of the Hamiltonian with respect to ψ_F requires knowledge of the fermion distribution functions. These distribution functions have no classical analog; however, Iwamoto and Yamada⁸ and Wu and Feenberg⁹ developed a cluster-expansion technique for calculating the distribution functions and, in general, those expectation values taken with respect to ψ_F . This expansion is known as the statistical cluster expansion since it is the antisymmetrizer of Eq. (1.2) which is approximated. In each order of the cluster expansion the product of pair functions is kept intact. Thus, order by order one requires only the boson distribution functions. In particular, by truncating the cluster series for the energy after the third term and using approximate forms for the three-body distribution function one can write the fermion energy as a functional of the associated boson two-body distribution function only.

Thus, both boson and fermion energies are determined by the two-body distribution functions generated by ψ_B . In this paper we shall discuss distribution functions obtained by solving the Born-Bogoliubov-Green-Kirkwood-Yvon¹⁰ (BBGKY) integral equation with the Kirkwood superposition approximation¹¹ (KSA) closure and compare them with distribution functions obtained as solutions of the hypernetted-chain (HNC) integral equation³ and the molecular-dynamics results of Schiff and Verlet.² In Sec. II we write down the equations which we shall use and review the method of calculation.

In Secs. III and IV we discuss the results obtained for ${}^4\text{He}$ and ${}^3\text{He}$, respectively, and Sec. V is then devoted to a discussion of the results. In Appendix A we discuss the details of the numerical solutions of the BBGKY-KSA and HNC integral equations. In Appendix B we discuss a point with regard to the statistical cluster expansion of the fermion number density and in Appendix C we give some numerical results of the effect on the BBGKY-KSA energy of adding zero-point phonons to the wave function.

II. METHOD OF CALCULATION

We consider N particles in a box of volume Ω in the limit that $N, \Omega \rightarrow \infty$, while the number density $\rho = N/\Omega$ remains a constant. The system is described by a Hamiltonian, H , where

$$H = -\frac{\hbar^2}{2m} \sum_{i=1}^N \nabla_i^2 + \sum_{j>i=1}^N v(r_{ij}) \quad (2.1)$$

and the two-body interaction is taken to be a Lennard-Jones form with the DeBoer-Michels parameters

$$v(r) = 4\epsilon [(\sigma/r)^{12} - (\sigma/r)^6], \quad (2.2)$$

and

$$\epsilon = 10.22^\circ\text{K}, \quad \sigma = 2.556 \text{ \AA}. \quad (2.3)$$

It is useful to use reduced units, denoted by an asterisk, where energies are measured in units of ϵ and lengths are measured in units of σ . Then the reduced Hamiltonian, H^* , is written

$$H^* = -\frac{1}{2}\eta \sum_i \nabla_i^{*2} + \sum_{j>i} v^*(r_{ij}^*), \quad (2.4)$$

where

$$\eta \equiv \hbar^2/m\epsilon\sigma^2 \quad (2.5)$$

and

$$r^* = r/\sigma. \quad (2.6)$$

The quantum parameter η is 0.2409 for ${}^3\text{He}$ and 0.1815 for ${}^4\text{He}$.

We chose the pair function $u(r)$ to have the parametric form

$$u(r) = -(b\sigma/r)^5 = -(b/r^*)^5 \quad (2.7)$$

in both Bose and Fermi systems. For a pair function with this simple power-law form and a pair potential which is just a sum of simple powers, a scaling procedure is available which greatly simplifies the calculation of the minimum energy expectation values. This property was first used by McMillan¹ in his study of ${}^4\text{He}$ and can be simply presented by introducing lengths scaled in units of $b\sigma$:

$$R = r/b\sigma = r^*/b, \quad (2.8)$$

$$D = \rho\sigma^3 b^3 = \rho^* b^3. \quad (2.9)$$

It is straightforward to show that the averages one needs for the energy E^* are functions of D and the particular statistics only. Thus the energy can be written in the simple form

$$E_x^*(\rho^*, \eta; b) = \frac{\eta}{b^2} \langle \frac{t}{N} \rangle_{D,x} + \frac{4}{b^{12}} \langle \frac{1}{R^{12}} \rangle_{D,x} - \frac{4}{b^6} \langle \frac{1}{R^6} \rangle_{D,x}, \quad (2.10)$$

where x stands for Bose or Fermi. The angular brackets represent averages defined by

$$\langle \frac{1}{R^N} \rangle_{D,x} = \frac{D}{2} \int g_x(R; D) \frac{1}{R^N} d\vec{R}, \quad (2.11)$$

$$\langle \frac{t}{N} \rangle_{D,x} = -\frac{1}{2N} \sum_{i=1}^N \frac{\int \psi_x^* \nabla_i^2 \psi_x d\vec{R}^N}{\int |\psi_x|^2 d\vec{R}^N}, \quad (2.12)$$

and in particular $\langle t/N \rangle_{D,B} = 5\langle 1/R^7 \rangle_D$. The $g_x(R; D)$ are Bose or spin-averaged Fermi radial distribution functions defined by

$$g_x(R_{12}; D) = \frac{N(N-1)}{D^2} \frac{\int \psi_x^2 d\vec{R}_3 \cdots d\vec{R}_N}{\int |\psi_x|^2 d\vec{R}_1 \cdots d\vec{R}_N}. \quad (2.13)$$

The fact that the energy can be written in the form of Eq. (2.10) has the important consequence that pressures calculated by differentiating E_x^* with respect to volume:

$$P^* = \rho^{*2} \frac{dE^*}{d\rho^*} \quad (2.14)$$

are consistent with the virial theorem.¹² This is simply shown by differentiating Eq. (2.10) with respect to b at constant D . Then, using the chain rule and the fact that b is a variational parameter one finds

$$P^* = \frac{2}{3} \rho^* (\epsilon_{KE} - 3\epsilon_6 + 6\epsilon_{12}), \quad (2.15)$$

where P^* is given by Eq. (2.14) and we have separated the energy into its constituents:

$$\epsilon_{KE} = (\eta/b^2) \langle t/N \rangle_{x,D}, \quad (2.16)$$

$$\epsilon_6 = (4/b^6) \langle 1/R^6 \rangle_{x,D}, \quad (2.17)$$

$$\epsilon_{12} = (4/b^{12}) \langle 1/R^{12} \rangle_{x,D}. \quad (2.18)$$

The right-hand side of Eq. (2.15) is the virial-theorem pressure.¹³

The fermion kinetic energy and radial distribution function are calculated approximately by using the statistical cluster procedure of Wu and Feenberg.⁹ Thus, for $g_F(R; D)$ we have

$$g_F(R_{12}; D) = g_B(R_{12}; D) + \Sigma^{(2)}(R_{12}; D) + \Sigma^{(3)}(R_{12}; D) + \cdots, \quad (2.19)$$

where

$$\Sigma^{(2)}(R_{12}; D) = -\frac{1}{2} g_B(R_{12}; D) l^2(Y_{12}), \quad (2.20)$$

$$\Sigma^{(3)}(R_{12}; D) = g_B(R_{12}; D) \left(-D \int g_B(R_{23}; D) [h(R_{13}; D)] l^2(Y_{23}) d\vec{R}_3 + \frac{1}{2} D l(Y_{12}) \int g_B(R_{23}; D) \right. \\ \left. \times [h(R_{13}; D)] l(Y_{13}) l(Y_{23}) d\vec{R}_3 \right) \quad (2.21)$$

and we have defined the following quantities:

$$h(R) = g(R) - 1, \quad (2.22)$$

$$l(Y_{12}) = 3[\sin(Y_{12}) - Y_{12} \cos(Y_{12})]/Y_{12}^3, \quad (2.23)$$

$$Y_{12} = k_D R_{12}, \quad (2.24)$$

$$k_D = (3\pi^2 D)^{1/3}. \quad (2.25)$$

The n th term in Eq. (2.19) represents the contribution to $g_F(R)$ coming from n -particle exchange in the Slater determinant. In order to evaluate $\Sigma^{(3)}$ the Kirkwood superposition approximation (KSA) has been used for the three-particle distribution function; i.e.,

$$p_{\text{KSA}}^{(3)}(1, 2, 3) = D^3 g_B(R_{12}; D) g_B(R_{13}; D) g_B(R_{23}; D). \quad (2.26)$$

The series in Eq. (2.19) is truncated after the third term. The one-parameter form chosen for $u(r)$ thus allows us to calculate a single set of $g_B(R)$'s as functions of D alone. These can then be used at an arbitrary density with a variational parameter, b , given by Eq. (2.9).

The cluster expansion for the fermion kinetic energy yields

$$\langle t/N \rangle_{D,F} = 5 \langle 1/R^7 \rangle_{D,F} + E_{1F} + E_{2F} + E_{3F} + \dots, \quad (2.27)$$

where

$$E_{1F} = \frac{3}{10} k_D^2, \quad (2.28)$$

$$E_{2F} = 20 E_{1F} \int_0^1 u(2k_D x) (1 - \frac{3}{2}x + \frac{1}{2}x^3) x^4 dx, \quad (2.29)$$

$$E_{3F} = -\frac{5}{6} E_{1F} \left(\frac{3}{8\pi} \right)^3 \int x_{12}^2 S(x_{12} k_D) u(x_{23} k_D) u(x_{13} k_D) \\ \times d\vec{x}_1 d\vec{x}_2 d\vec{x}_3, \quad (2.30)$$

and

$$u(k) = S(k) - 1 = D \int e^{i\vec{k} \cdot \vec{R}} h(R; D) d\vec{R}. \quad (2.31)$$

Following Wu and Feenberg, we have used the convolution approximation for the three-particle distribution function in E_{3F} , where

$$p_{\text{CA}}^{(3)}(1, 2, 3) = D^3 [1 + h(R_{12}; D) + h(R_{23}; D) + h(R_{31}; D) \\ + h(R_{12}; D) h(R_{23}; D) \\ + h(R_{12}; D) h(R_{31}; D) \\ + h(R_{23}; D) h(R_{31}; D)] \\ + D \int h(R_{14}; D) h(R_{24}; D) h(R_{34}; D) d\vec{R}_4. \quad (2.32)$$

A quadratic approximation to $S(k)^{14}$ was employed in order to evaluate E_{3F} (the integrations are over unit spheres).

The boson $g(R)$'s were obtained by solution of the BBGKY and HNC integral equations. The BBGKY equation is given by

$$\vec{\nabla}_1 g(R_{12}; D) = \vec{\nabla}_1 u(R_{12}) g(R_{12}; D) \\ + D \int \frac{p^{(3)}(1, 2, 3)}{D^3} \vec{\nabla}_1 u(R_{13}) d\vec{R}_3, \quad (2.33)$$

and is obtained by applying the gradient operator to the definition of $g(R)$ [Eq. (2.13)]. The KSA approximation, [Eq. (2.26)], has been used for the three-body distribution function. The HNC equation is defined by the Ornstein-Zernike equation:

$$h(R) = C(R) + D \int d\vec{S} C(S) h(|\vec{R} - \vec{S}|) \quad (2.34)$$

together with the direct correlation function,

$$C(R) = h(R) - \ln[g(R)/e^{u(R)}]. \quad (2.35)$$

The details of the solutions of these equations are discussed in Appendix A.

In Table I (II) we show the Bose and Fermi averages as defined in Eqs. (2.11) and (2.12) for the BBGKY (HNC) $g(R)$'s. The averages are smooth and monotonic and slowly varying over a large range in D . We can thus fit these averages as cubic polynomials in D rather accurately and obtain explicit expressions for the Bose and Fermi energies as functions of ρ^* , η , and b . The equations of state will be obtained by analyzing the curve-fit polynomials. We define the polynomial coefficients as follows:

$$\left\langle \frac{t}{N} \right\rangle_{D,x} = \alpha_{0,x} D^{2/3} + \sum_{i=1}^3 \alpha_{i,x} D^i, \quad (2.36)$$

$$\left\langle \frac{1}{R^6} \right\rangle_{D,x} = \sum_{i=1}^3 \beta_{i,x} D^i, \quad (2.37)$$

$$\left\langle \frac{1}{R^{12}} \right\rangle_{D,x} = \sum_{i=1}^3 \gamma_{i,x} D^i, \quad (2.38)$$

with

$$\alpha_{0,x} = \begin{cases} 2.7(\frac{1}{3}\pi)^{4/3}, & x = F \\ 0, & x = B \end{cases}. \quad (2.39)$$

In the fermion kinetic-energy term we have separated off E_{1F} the average independent-particle kinetic energy which is independent of b .

TABLE I. Components of E^* for ${}^3\text{He}$ and ${}^4\text{He}$ for the BBGKY-KSA data. Averages are defined in Eqs. (2.11) and (2.12); $\langle t/N \rangle_F^\dagger = \langle t/N \rangle_F - \frac{3}{10}k_D^2$.

D	$\langle t/N \rangle_F^\dagger$	$\langle R^{-6} \rangle_F$	$\langle R^{-12} \rangle_F$	$\langle t/N \rangle_B$	$\langle R^{-6} \rangle_B$	$\langle R^{-12} \rangle_B$
0.050	0.268	0.076	0.044	0.404	0.101	0.066
0.100	0.646	0.180	0.109	0.884	0.220	0.151
0.150	1.113	0.304	0.195	1.443	0.354	0.257
0.200	1.665	0.445	0.302	2.080	0.504	0.385
0.225	1.972	0.522	0.364	2.429	0.585	0.458
0.250	2.299	0.603	0.433	2.797	0.669	0.537
0.275	2.647	0.688	0.507	3.185	0.758	0.623
0.300	3.015	0.776	0.588	3.593	0.850	0.716
0.325	3.404	0.869	0.676	4.021	0.945	0.816
0.350	3.812	0.965	0.770	4.468	1.045	0.923
0.375	4.241	1.065	0.872	4.935	1.148	1.037
0.400	4.690	1.168	0.981	5.422	1.254	1.159
0.425	5.159	1.275	1.097	5.928	1.364	1.289
0.450	5.648	1.386	1.221	6.454	1.478	1.427
0.475	6.156	1.500	1.353	6.999	1.595	1.573
0.500	6.685	1.618	1.493	7.562	1.715	1.727
0.550	7.800	1.864	1.798	8.747	1.965	2.059
0.600	8.991	2.123	2.135	10.005	2.228	2.426
0.625	9.615	2.258	2.317	10.661	2.365	2.622
0.650	10.258	2.395	2.507	11.335	2.504	2.826
0.675	10.918	2.536	2.705	12.026	2.646	3.038
0.700	11.597	2.680	2.912	12.734	2.791	3.259
0.725	12.292	2.827	3.126	13.459	2.939	3.488
0.750	13.005	2.977	3.349	14.199	3.089	3.725
0.775	13.733	3.129	3.580	14.955	3.242	3.969
0.800	14.478	3.284	3.819	15.726	3.398	4.221
0.850	16.014	3.603	4.319	17.310	3.716	4.745
0.900	17.606	3.931	4.846	18.947	4.043	5.295
0.950	19.251	4.268	5.398	20.631	4.378	5.867
1.000	20.942	4.613	5.970	22.356	4.720	6.455
1.050	22.673	4.966	6.557	24.114	5.068	7.054
1.100	24.437	5.326	7.151	25.898	5.421	7.656

III. RESULTS FOR ${}^4\text{He}$

In this section we shall calculate the energies and pressures for ${}^4\text{He}$ using the data of Tables I and II. The integral-equation results will be compared to the molecular-dynamics (MD) results of Schiff and Verlet (SV) and experiment.

If we use Eqs. (2.10) and (2.36)–(2.38), the ${}^4\text{He}$ ($\eta=0.1815$) energy can be written

$$E^*(\rho^*; b) = \sum_{n=1}^3 D^n (\eta b^{-2} \alpha_n - 4b^{-6} \beta_n + 4b^{-12} \gamma_n). \quad (3.1)$$

The variational parameter b is determined by

$$\left(\frac{\partial E^*}{\partial b} \right)_{\rho^*} = 0 = b^{-1} \sum_{n=1}^3 D^n [(3n-2)b^{-2} \alpha_n - 12(n-2)b^{-6} \beta_n + 12(n-4)b^{-12} \gamma_n]. \quad (3.2)$$

Using Eq. (3.1) the pressure is given by

$$P^*(\rho^*) = \rho^* \sum_{n=1}^3 n D^n (\eta b^{-2} \alpha_n - 4b^{-6} \beta_n + 4b^{-12} \gamma_n). \quad (3.3)$$

The coefficients $\alpha_n, \beta_n, \gamma_n$ ($n=1, 2, 3$) were obtained by means of a Chebyshev curve fit¹⁵ of the data in Tables I and II. These coefficients are displayed in Tables III and IV for the BBGKY and HNC data, respectively. For the ${}^4\text{He}$ data there are two sets of coefficients in Tables III and IV corresponding to separate curve fits over a low-density and a high-density interval. This was found necessary in order to maintain three significant figure accuracy.

The energies and pressures thus obtained are shown in Figs. 1 and 2 and are displayed in Tables V and VI. The distinctive feature of these curves is how “soft” the BBGKY equation of state is relative to the HNC and MD results. HNC results for ${}^4\text{He}$ were previously reported by Murphy and Watts³ (MW) (our present results are in excellent agreement with MW: the energies differ by approximately $0.005\epsilon^\circ\text{K}$ in the density range shown in Fig. 1). The crosses in Fig. 1 are the “experimental” energies calculated by MW by numerical integration of the experimental pressure data of Boghosian and Meyer.¹⁶ It is clear that for

TABLE II. Components of E^* for ^3He and ^4He for the HNC data. Averages are defined in Eqs. (2.11) and (2.12); $\langle t/N \rangle_F^+ = \langle t/N \rangle_F - \frac{3}{10}k_D^2$.

D	$\langle t/N \rangle_F^+$	$\langle R^{-6} \rangle_F$	$\langle R^{-12} \rangle_F$	$\langle t/N \rangle_B$	$\langle R^{-6} \rangle_B$	$\langle R^{-12} \rangle_B$
0.050	0.269	0.076	0.044	0.405	0.102	0.067
0.075	0.449	0.126	0.075	0.640	0.160	0.108
0.100	0.655	0.182	0.111	0.896	0.222	0.155
0.125	0.885	0.243	0.154	1.175	0.289	0.208
0.150	1.141	0.309	0.202	1.478	0.361	0.267
0.175	1.421	0.381	0.257	1.805	0.437	0.334
0.200	1.726	0.457	0.320	2.156	0.519	0.409
0.225	2.057	0.538	0.390	2.532	0.604	0.492
0.250	2.414	0.624	0.469	2.933	0.695	0.583
0.275	2.796	0.714	0.556	3.359	0.790	0.685
0.300	3.204	0.810	0.652	3.812	0.890	0.796
0.325	3.639	0.910	0.759	4.290	0.995	0.918
0.350	4.101	1.015	0.876	4.795	1.104	1.051
0.375	4.590	1.125	1.004	5.327	1.218	1.196
0.400	5.106	1.240	1.144	5.885	1.336	1.353
0.425	5.650	1.359	1.296	6.471	1.459	1.524
0.450	6.221	1.483	1.461	7.085	1.587	1.708
0.475	6.821	1.612	1.640	7.726	1.720	1.907
0.500	7.449	1.745	1.834	8.396	1.857	2.121
0.525	8.106	1.883	2.043	9.094	1.999	2.351
0.550	8.791	2.026	2.267	9.820	2.145	2.597
0.582	9.720	2.218	2.582	10.801	2.341	2.941
0.600	10.238	2.324	2.760	11.347	2.450	3.135
0.625	11.010	2.481	3.035	12.159	2.610	3.435
0.650	11.812	2.642	3.329	13.000	2.774	3.754
0.675	12.644	2.808	3.643	13.871	2.943	4.093
0.700	13.505	2.979	3.977	14.772	3.117	4.453
0.725	14.397	3.154	4.332	15.703	3.295	4.835
0.750	15.320	3.334	4.709	16.664	3.478	5.240

$\rho^* \geq 0.4$ the BBGKY-KSA energies are *lower* than experiment. In Fig. 2 we have plotted pressure as a function of the difference in density from the zero-pressure density, ρ_0^* . The crosses are the experimental data of Boghosian and Meyer. The HNC pressures are clearly superior to the BBGKY-KSA. Further, it appears from inspection

of Fig. 1 that the MD results should give rather good pressures as the slopes seem to be in good agreement with HNC at a *higher* density. In Fig. 3 we show the optimal variational parameter at each density as determined by Eq. (3.2). (The difference in energy across the gaps of the two curve-fits for the HNC and BBGKY data are 0.0003 and

TABLE III. Coefficient for the polynomial fits to the BBGKY-KSA averages given in Table I. The coefficients are defined in Eqs. (2.36)–(2.39).

Coefficient	^4He		^3He
	$0.26 \leq \rho^* \leq 0.36^a$	$0.34 \leq \rho^* \leq 0.50^b$	$0.15 \leq \rho^* \leq 0.40^c$
α_1	7.041	6.529	4.785
α_2	16.743	18.476	18.090
α_3	-1.143	-2.591	-1.828
β_1	1.859	1.810	1.464
β_2	3.398	3.564	4.028
β_3	-0.510	-0.647	-0.956
γ_1	0.995	0.532	0.734
γ_2	4.115	5.679	3.472
γ_3	1.605	0.303	2.062

^a These coefficients were determined by fitting the data in the interval $D \in [0.40, 0.65]$ in Table I.

^b Same as above with $D \in [0.50, 0.90]$.

^c Same as above with $D \in [0.20, 0.60]$.

TABLE IV. Coefficients for the polynomial fit to the HNC averages given in Table II. Coefficients are defined in Eqs. (2.36)–(2.39).

Coefficient	⁴ He		³ He
	0.21 ≤ ρ* ≤ 0.36 ^a	0.29 ≤ ρ* ≤ 0.42 ^b	0.12 ≤ ρ* ≤ 0.30 ^c
α ₁	6.923	6.972	4.601
α ₂	18.504	18.305	19.865
α ₃	2.487	2.682	1.385
β ₁	1.817	1.839	1.391
β ₂	3.882	3.793	4.648
β ₃	-0.172	-0.084	-0.937
γ ₁	1.181	1.391	0.776
γ ₂	3.041	2.188	3.024
γ ₃	6.180	7.021	5.478

^a These coefficients were determined by fitting the data in the interval $D \in [0.30, 0.60]$ in Table II.

^b Same as above with $D \in [0.40, 0.75]$.

^c Same as above with $D \in [0.15, 0.45]$.

0.001ε °K, respectively.) The cross in Fig. 3 is the value of b found by SV at the zero-pressure MD energy.

In Fig. 4 we compare the radial-distribution functions of the BBGKY-KSA, HNC, and MD calculations. The good agreement between the HNC and MD $g(r)$'s is evident and was noted by MW. The BBGKY-KSA is obviously the odd-man-out. In the important region around the initial rise it lies significantly under the HNC and MD curves. It then peaks too far out and returns to 1.0 too slowly. The KSA overcorrelates; it is too good at keeping the particles out of their neighbor's repulsive cores.

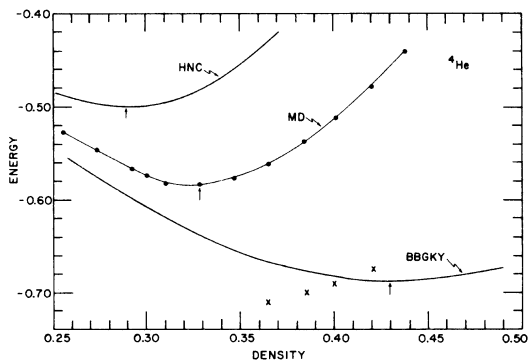


FIG. 1. Energy as a function of density for ⁴He comparing the BBGKY-KSA, HNC, and molecular-dynamics results. Arrows locate the minima in the curves. Crosses are the "experimental" energies as calculated by Murphy and Watts. All quantities are measured in reduced units. Line through the MD points is a guide to the eye.

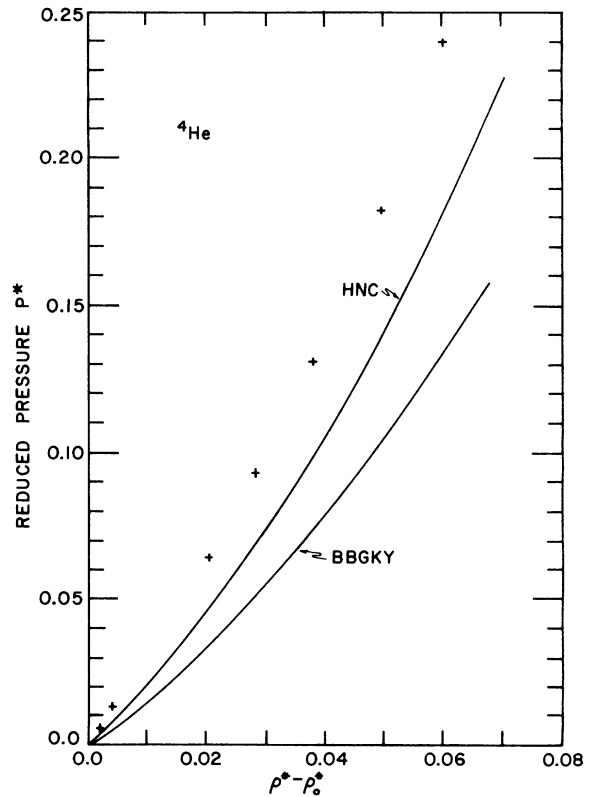


FIG. 2. Pressure as a function of the density as measured from ρ_0^* , the zero-pressure density, for ⁴He. We compare the HNC and BBGKY-KSA results with the experimental data of Boghosian and Meyer (crosses). All quantities are measured in reduced units. ρ_0^* (expt.) = 0.3648, ρ_0^* (BBGKY-KSA) = 0.43, ρ_0^* (HNC) = 0.29. Unit reduced pressure is equivalent to 84.5 bar.

TABLE V. Energies and pressures for ^4He calculated from the BBGKY-KSA data. Energies are in units of ϵ and pressures are in units of ϵ/σ^3 .

ρ^*	E^*	b	ϵ_{KE}	ϵ_6	ϵ_{12}	P^*
0.27	-0.569	1.153	0.778	-2.239	0.892	-0.105
0.29	-0.597	1.157	0.872	-2.459	0.990	-0.109
0.31	-0.621	1.160	0.972	-2.687	1.094	-0.109
0.33	-0.642	1.164	1.076	-2.921	1.203	-0.103
0.35	-0.659	1.167	1.186	-3.164	1.318	-0.092
0.37	-0.670	1.170	1.303	-3.413	1.440	-0.072
0.39	-0.679	1.174	1.427	-3.663	1.558	-0.056
0.41	-0.685	1.178	1.556	-3.920	1.680	-0.034
0.43	-0.687	1.182	1.690	-4.184	1.807	-0.006
0.45	-0.686	1.185	1.829	-4.454	1.938	0.030
0.47	-0.681	1.188	1.973	-4.730	2.075	0.074
0.49	-0.672	1.191	2.121	-5.011	2.217	0.128

IV. RESULTS FOR ^3He

In this section we calculate the energies and pressures for ^3He using the statistical-cluster technique of Wu and Feenberg as discussed in Sec. II.

If we use Eqs. (2.10) and (2.36)–(2.39), the ^3He ($\eta=0.2409$) energy is written

$$E_F^*(\rho^*; b) = E_{1F}^* + \sum_{n=1}^3 D^n (\eta b^{-2} \alpha_n - 4b^{-6} \beta_n + 4b^{-12} \gamma_n), \quad (4.1)$$

where

$$E_{1F}^* = 2.7 \left(\frac{1}{3}\pi\right)^{4/3} \eta \rho^{*2/3} = \eta b^{-2} E_{1F}. \quad (4.2)$$

Since E_{1F}^* is independent of b , b is once more determined by Eq. (3.2),

$$\sum_{n=1}^3 D^n [(3n-2)\eta b^{-2} \alpha_n - 12(n-2)b^{-6} \beta_n + 12(n-4)b^{-12} \gamma_n] = 0. \quad (4.3)$$

TABLE VI. Energies and pressures for ^4He calculated from the HNC data. Energies are in units of ϵ and pressures are in units of ϵ/σ^3 .

ρ^*	E^*	b	ϵ_{KE}	ϵ_6	ϵ_{12}	P^*
0.21	-0.441	1.147	0.570	-1.687	0.676	-0.061
0.23	-0.466	1.151	0.659	-1.905	0.781	-0.057
0.25	-0.484	1.155	0.756	-2.133	0.894	-0.047
0.27	-0.495	1.159	0.860	-2.372	1.017	-0.028
0.29	-0.499	1.163	0.971	-2.621	1.151	0.003
0.31	-0.494	1.166	1.091	-2.880	1.295	0.046
0.33	-0.480	1.170	1.219	-3.150	1.451	0.105
0.35	-0.455	1.173	1.355	-3.429	1.619	0.182
0.37	-0.420	1.176	1.496	-3.725	1.810	0.291
0.39	-0.371	1.179	1.648	-4.027	2.008	0.420
0.41	-0.309	1.182	1.811	-4.340	2.220	0.577

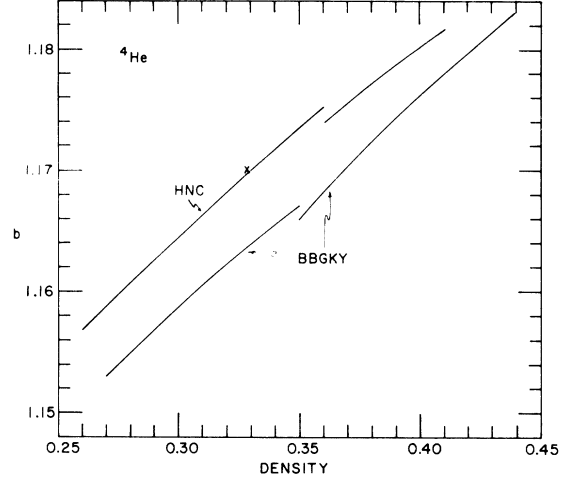


FIG. 3. ^4He variational parameter at each density as determined by the HNC and BBGKY-KSA equations. As indicated in Tables III and IV, two curve fits were used to cover the density range. Cross is the value of b that ρ_0^* (BBGKY-KSA) = 0.273, ρ_0^* (HNC) = 0.21. Unit reduced pressure is equivalent to 84.5 bar.

The pressure is given by Eqs. (4.1) and (2.14),

$$P_F^*(\rho^*) = P_{1F}^* + \rho^* \sum_{n=1}^3 n D^n (\eta b^{-2} \alpha_n - 4b^{-6} \beta_n + 4b^{-12} \gamma_n), \quad (4.4)$$

where

$$P_{1F}^* = \frac{2}{3} \rho^* E_{1F}^*. \quad (4.5)$$

The ^3He α , β , and γ coefficients determined by fitting the data in Table I and II are shown in Tables III and IV for the BBGKY-KSA and HNC, respectively. Because of the lower density of ^3He one set of coefficients is sufficient to cover the density range of interest.

In Figs. 5 and 6 we show the energies and pressures for ^3He as calculated with Eqs. (4.1)–(4.5)

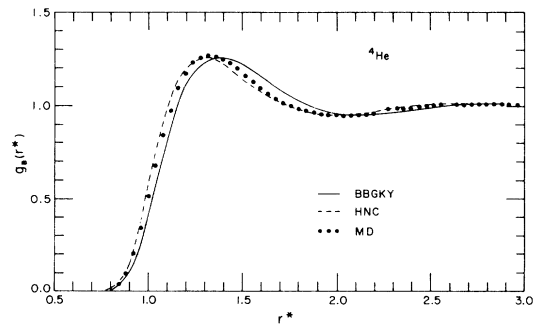


FIG. 4. Radial distribution functions for ^4He at the experimental ground-state density = $0.3648/\sigma^3 \text{ \AA}^{-3}$. Molecular-dynamics result is compared to the HNC and BBGKY-KSA $g_B(r^*)$'s at $D=0.60$.

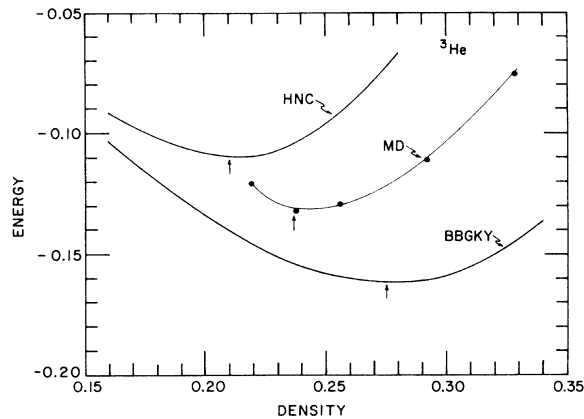


FIG. 5. Energy as a function of density for ${}^3\text{He}$ comparing the BBGKY-KSA, HNC, and molecular-dynamics results. Arrows locate the minima in the curves. Line through the MD points is a guide to the eye. All quantities are measured in reduced units. Experimental energy is -0.245ϵ at a density of $0.273\sigma^3$ and zero pressure.

and in Tables VII and VIII we display the data. In Fig. 5 we see that, as in the case of ${}^4\text{He}$, the BBGKY-KSA equation of state is “softer” than either the HNC or MD equations of state; however, the disagreement among them is far less severe. The improved agreement is a result of the lower densities under consideration. As the density becomes smaller, the integral equations become more accurate and the results will be closer to MD. The ${}^3\text{He}$ pressure curves of Fig. 6 should be compared with the ${}^4\text{He}$ pressure curves of Fig. 2. The agreement between the integral-equation pressures for ${}^3\text{He}$ stands in marked contrast to their disagreement for ${}^4\text{He}$; however, neither integral-equation results compares well with the ${}^3\text{He}$ experimental pressures tabulated by Wheatley.¹⁷ P_{1F}^* (the pressure in a system of noninteracting fermions) is displayed in the last column of Tables VII and VIII.

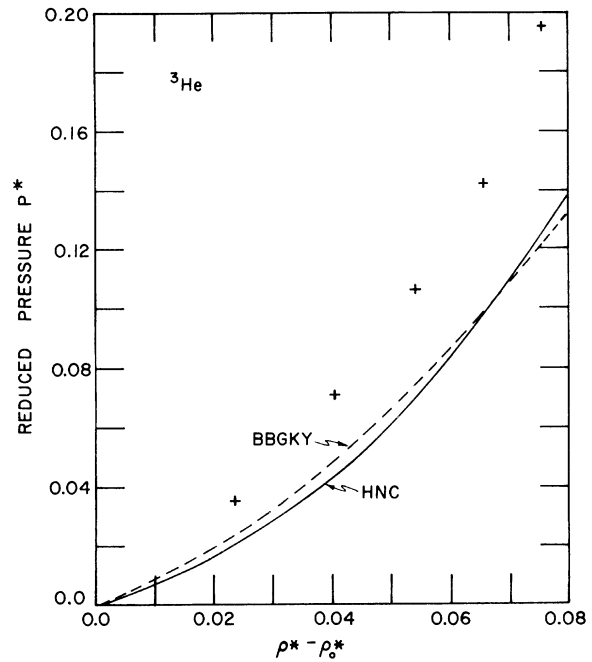


FIG. 6. Pressure as a function of density as measured from ρ_0^* , the zero-pressure density for ${}^3\text{He}$. We compare the HNC and BBGKY-KSA results with the experimental data compiled by Wheatley (crosses). All quantities are measured in reduced units. ρ_0^* (expt.) = 0.273, ρ_0^* (BBGKY-KSA) = 0.273, ρ_0^* (HNC) = 0.21. Unit reduced pressure is equivalent to 84.5 bar.

In Fig. 7 we show the variational parameter b as a function of density for the BBGKY-KSA and HNC data. These results are qualitatively similar to the ${}^4\text{He}$ results. At a given density the HNC equation minimizes the energy with a slightly larger value of the variational parameters than the BBGKY-KSA. The effect of Fermi statistics is to reduce the size of b since the antisymmetry acts like an effective repulsion and helps in keeping the particles out of each other’s strongly repulsive cores. (The b values for a Bose ${}^3\text{He}$ system can

TABLE VII. Energies and pressures for ${}^3\text{He}$ calculated from the BBGKY-KSA data. Energies are in units of ϵ and pressures are in units of ϵ/σ^3 .

ρ^*	E^*	b	E_{1F}^*	ϵ_{KE}	ϵ_6	ϵ_{12}	P^*	P_{1F}^*
0.19	-0.127	1.110	0.229	0.704	-1.360	0.529	-0.026	0.0290
0.21	-0.141	1.113	0.244	0.801	-1.553	0.612	-0.026	0.0342
0.23	-0.151	1.117	0.260	0.903	-1.755	0.702	-0.023	0.0398
0.25	-0.158	1.120	0.274	1.010	-1.966	0.798	-0.017	0.0457
0.27	-0.162	1.123	0.289	1.123	-2.186	0.901	-0.005	0.0520
0.29	-0.161	1.125	0.303	1.242	-2.414	1.012	0.013	0.0586
0.31	-0.155	1.128	0.317	1.367	-2.651	1.129	0.039	0.0655
0.33	-0.144	1.130	0.330	1.497	-2.896	1.254	0.074	0.0727
0.35	-0.128	1.132	0.344	1.633	-3.148	1.387	0.120	0.0802
0.37	-0.105	1.134	0.356	1.774	-3.408	1.528	0.178	0.0879
0.39	-0.0756	1.136	0.369	1.922	-3.675	1.678	0.250	0.0960

TABLE VIII. Energies and pressures for ${}^3\text{He}$ calculated from the HNC data. Energies are in units of ϵ and pressures are in units of ϵ/σ^3 .

ρ^*	E^*	b	E_{1F}^*	ϵ_{KE}	ϵ_6	ϵ_{12}	P^*	P_{1F}^*
0.15	-0.0846	1.106	0.195	0.5426	-1.0185	0.3913	-0.017	0.0195
0.17	-0.0976	1.110	0.212	0.6343	-1.2053	0.4734	-0.016	0.0241
0.19	-0.106	1.113	0.229	0.7327	-1.4037	0.5647	-0.011	0.0290
0.21	-0.110	1.116	0.244	0.8380	-1.6134	0.6656	-0.001	0.0342
0.23	-0.107	1.119	0.260	0.9504	-1.8343	0.7767	0.016	0.0398
0.25	-0.0970	1.122	0.274	1.0703	-2.0661	0.8987	0.044	0.0457
0.27	-0.0786	1.124	0.289	1.1977	-2.3085	1.0322	0.084	0.0520
0.29	-0.0508	1.127	0.303	1.3330	-2.5614	1.1776	0.14	0.0586

be obtained by shifting the curves in Fig. 7 upward by an approximately constant additive factor of 0.015.)

The fermion radial-distribution functions, $g_F(r^*)$, for the BBGKY-KSA, HNC, and MD calculations at the ${}^3\text{He}$ experimental (reduced) density, 0.273, are shown in Fig. 8. The $g_F(r^*)$ are calculated by the statistical cluster expansion as given in Eqs. (2.19)–(2.21). As already implied by the energies, these $g_F(r^*)$'s are in much better agreement than the $g_B(r^*)$'s for ${}^4\text{He}$. The BBGKY-KSA $g_F(r^*)$ has the same problems as the $g_B(r^*)$ from which it is generated: it rises too slowly and peaks too far out. The HNC $g_F(r^*)$ shows good agreement with MD.

In the spirit of the statistical cluster expansion we write the ground-state energy as

$$E_F^* = E_1 + E_2 + E_3 + \dots, \quad (4.6)$$

where E_α ($\alpha \geq 2$) represents the contribution from α -body exchange in the Slater determinant of ψ_F ,

[Eq. (1.2)]. Thus we have for the first term in the cluster expansion

$$E_1 = E_{1F}^* + E_B^*, \quad (4.7)$$

where E_B^* is the energy generated by just the ψ_B portion of ψ_F . We note that this is *not* the same ordering as used by Woo¹⁴ or SV. SV placed E_{1F}^* in the *second* term of the cluster expansion, E_2 . Woo used a slightly different wave function, in principle, by choosing ψ_B to be an eigenfunction of a fictitious ${}^3\text{He}$ Boson system. Then E_B^* is the eigenvalue of ψ_B and there are no other contributions from integrations over the potential energy. The two-body and three-body terms are given by Eqs. (2.29) and (2.30). Thus, the series as ordered by Woo is

$$E = \tilde{E}_0 + \tilde{E}_1 + \tilde{E}_2 + \tilde{E}_3, \quad (4.8)$$

where

$$\tilde{E}_0 = E_B^*, \quad \tilde{E}_1 = E_{1F}^*, \quad \tilde{E}_2 = 2\eta b^{-2} E_{2F}, \quad \tilde{E}_3 = 2\eta b^{-2} E_{3F}. \quad (4.9)$$

In the ordering scheme of Eq. (4.7) the first approximation to the fermion wave function is given by ψ_B times a product of plane waves and spin factors, (a correlated Hartree), whereas SV and Woo

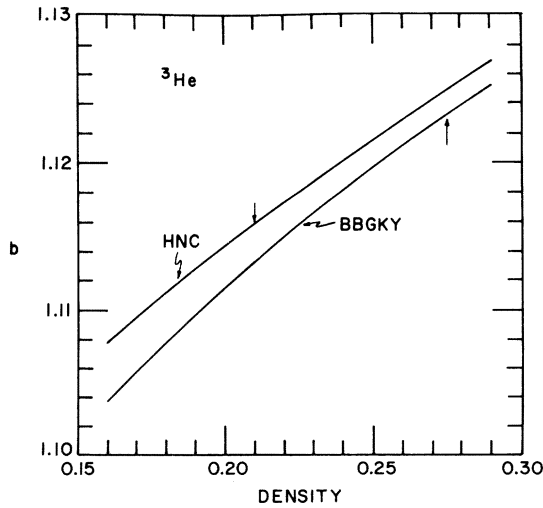


FIG. 7. ${}^3\text{He}$ variational parameter at each density as determined in the BBGKY-KSA and HNC approximations. Arrows locate the zero-pressure densities.

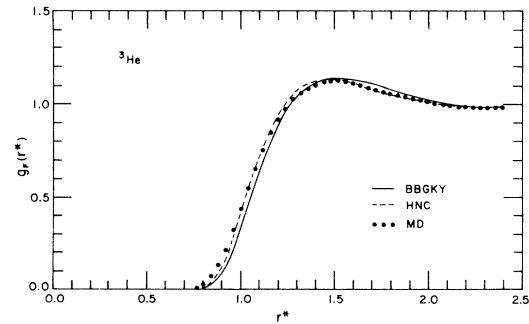


FIG. 8. Radial-distribution functions for ${}^3\text{He}$ at the experimental ground-state density $= 0.273/\sigma^3 \text{ \AA}^{-3}$. Molecular-dynamics result of Schiff and Verlet is compared to the BBGKY-KSA and HNC $g_F(r^*)$'s at $D=0.40$.

TABLE IX. ${}^3\text{He}$ energies for the BBGKY-KSA data arranged order by order in the statistical cluster expansion as defined in Eqs. (4.6), (4.7), and (4.10).

ρ^*	E_1	E_2	$E_1 + E_2$	E_3	E_3/E_2
0.19	-0.048	-0.067	-0.115	-0.014	0.20
0.21	-0.048	-0.079	-0.128	-0.014	0.18
0.23	-0.045	-0.093	-0.137	-0.015	0.16
0.25	-0.038	-0.106	-0.144	-0.015	0.14
0.27	-0.026	-0.120	-0.146	-0.015	0.13
0.29	-0.010	-0.135	-0.144	-0.016	0.12
0.31	0.012	-0.149	-0.138	-0.016	0.11
0.33	0.038	-0.165	-0.126	-0.016	0.10
0.35	0.070	-0.180	-0.110	-0.016	0.09
0.37	0.108	-0.196	-0.088	-0.016	0.08
0.39	0.152	-0.212	-0.060	-0.015	0.07

use ψ_B alone. We prefer E_1 of Eq. (4.7) for two reasons: (i) it has the correct noninteracting limit (in the spirit of the cluster expansion) and (ii) it has the correct low-density (Hartree) behavior. This is especially evident for systems with small values of η wherein E_{1F}^* is the dominant contribution to the energy. Thus, E_1 is a fermion system in approximation and not just a boson system.

The succeeding terms in the cluster expansion are given by

$$E_\alpha = \frac{\rho^*}{2} \int \Sigma^{(\alpha)}(r^*) \bar{v}(r^*) d\bar{\Gamma}^* + \eta b^{-2} E_{\alpha F}, \quad (4.10)$$

with $\alpha = 2, 3, 4, \dots$. The $\Sigma^{(\alpha)}(r^*)$ and $E_{\alpha F}$ for $\alpha = 2, 3$ are defined in Eqs. (2.20), (2.21), (2.29), and (2.30) also

$$\bar{v}(r) = v(r) - \frac{1}{4} \eta \nabla^2 u(r). \quad (4.11)$$

In Fig. 8 we show the ${}^3\text{He}$ energy components E_1 , E_2 , and E_3 for the BBGKY-KSA data. Further, in Tables IX and X the E_1 , E_2 , and E_3 for both the HNC and BBGKY-KSA are listed. Figure 9 and its tables show the very important result that the ${}^3\text{He}$ energy minimizes at a density close to the density at which E_1 tends to *vanish*. Thus, at the zero-pressure density 80% of the total energy is

TABLE X. ${}^3\text{He}$ energies for the HNC data arranged order by order in the statistical cluster expansion as defined in Eqs. (4.6), (4.7), and (4.10).

ρ^*	E_1	E_2	$E_1 + E_2$	E_3	E_3/E_2
0.15	-0.028	-0.046	-0.074	-0.011	0.24
0.17	-0.027	-0.059	-0.086	-0.012	0.20
0.19	-0.021	-0.073	-0.095	-0.012	0.16
0.21	-0.009	-0.089	-0.098	-0.012	0.13
0.23	0.010	-0.105	-0.096	-0.011	0.11
0.25	0.037	-0.123	-0.086	-0.010	0.08
0.27	0.073	-0.142	-0.069	-0.009	0.06
0.29	0.119	-0.162	-0.043	-0.007	0.05

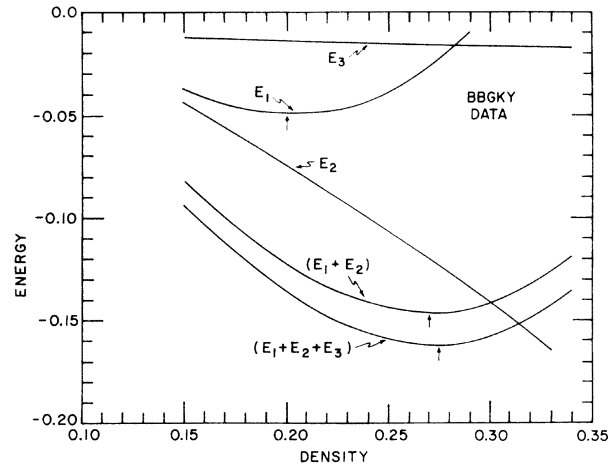


FIG. 9. ${}^3\text{He}$ energy vs density for the BBGKY-KSA data with each order of the statistical cluster expansion displayed separately.

contributed by E_2 , the two-body exchange contribution. When the energies of Woo and SV are ordered with the correlated Hartree, E_1 , as the first term in the cluster expansion similar results are obtained. In Fig. 10 we show the ratio of E_3 to E_2 as a function of density. We note that this ratio is quite small and that as the density increases E_3 will change sign. In Tables XI and XII we resolve the cluster energies, (E_1 , E_2 , and E_3) into their kinetic-energy and potential-energy parts. It is interesting to note that when the potential and kinetic energy are viewed separately the cluster expansion for each part appears to be rapidly

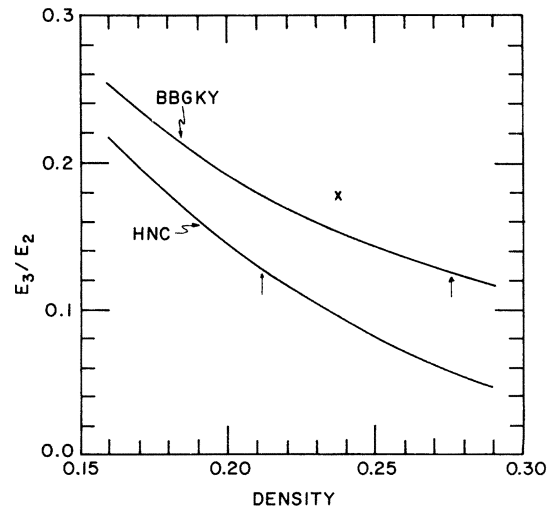


FIG. 10. Ratio E_3/E_2 of the ${}^3\text{He}$ cluster components for both the BBGKY-KSA and HNC energies as a function of density. Arrows locate the zero-pressure densities. Cross locates the ratio for MD at its zero-pressure density.

TABLE XI. ${}^3\text{He}$ cluster terms resolved into kinetic-energy and potential-energy components for the BBGKY-KSA data. Thus $E_\alpha = \epsilon_{\text{KE}}^{(\alpha)} + \epsilon_b^{(\alpha)} + \epsilon_{12}^{(\alpha)}$, $\alpha = 1, 2, 3$.

ρ^*	$\epsilon_{\text{KE}}^{(1)}$	$\epsilon_{\text{KE}}^{(2)}$	$\epsilon_{\text{KE}}^{(3)}$	$\epsilon_b^{(1)}$	$\epsilon_b^{(2)}$	$\epsilon_b^{(3)}$	$\epsilon_{12}^{(1)}$	$\epsilon_{12}^{(2)}$	$\epsilon_{12}^{(3)}$
0.19	0.805	-0.129	0.028	-1.507	0.223	-0.077	0.654	-0.161	0.036
0.21	0.910	-0.141	0.031	-1.706	0.237	-0.085	0.748	-0.175	0.039
0.23	1.021	-0.153	0.035	-1.914	0.250	-0.092	0.848	-0.190	0.043
0.25	1.137	-0.164	0.038	-2.130	0.262	-0.099	0.956	-0.204	0.046
0.27	1.258	-0.176	0.041	-2.354	0.274	-0.106	1.070	-0.218	0.049
0.29	1.385	-0.187	0.044	-2.586	0.285	-0.113	1.192	-0.233	0.052
0.31	1.518	-0.199	0.048	-2.827	0.297	-0.119	1.321	-0.247	0.055
0.33	1.656	-0.210	0.051	-3.075	0.307	-0.126	1.458	-0.262	0.059
0.35	1.800	-0.221	0.054	-3.331	0.317	-0.132	1.602	-0.276	0.062
0.37	1.949	-0.233	0.058	-3.595	0.327	-0.139	1.754	-0.291	0.065
0.39	2.104	-0.244	0.061	-3.867	0.336	-0.145	1.915	-0.305	0.069

converging.

The term-by-term convergence of the statistical cluster expansion, with the correlated Hartree energy as the first term, is not as methodical as in the ordering schemes of Woo and SV. From Tables VII–X one obtains the fact that $|E_B^*| > E_{1F}^* > |E_2|$ at ρ_0^* and thus it is clear how a different position for E_{1F}^* can result in a more systematically appearing convergence in the cluster series.

Finally, we would like to discuss the statistical cluster series for the fermion number density. The fermion radial distribution function can be written

$$g_F(r) = g_B(r) + \Sigma(r), \quad (4.12)$$

where $g_B(r)$ is the boson radial distribution function and $\Sigma(r)$ are the statistical cluster corrections. If we subtract unity from both sides of Eq. (4.12), integrate over \vec{r} , and use the sequential relations,¹⁸ we find

$$\frac{\rho_F}{\rho_B} = 1 + \sum_{\alpha=2}^N \rho_F^{(\alpha)}, \quad (4.13)$$

where

$$\rho_F^{(\alpha)} = \rho_F \int \Sigma^{(\alpha)}(\vec{r}) d\vec{r}, \quad (4.14)$$

and the α -body statistical cluster correction, $\Sigma^\alpha(r)$, for $\alpha = 2, 3$ has been written down in Eqs. (2.20)–(2.21). The number density is independent of statistics, thus we must have

$$\sum_{\alpha=2}^N \rho_F^{(\alpha)} = 0. \quad (4.15)$$

In Appendix B we discuss Eq. (4.15) with respect to a rigorous result due to Feenberg pertaining to the $\rho_F^{(\alpha)}$. In Fig. 11 we plot the ratio of $\rho_F^{(3)}$ to $\rho_F^{(2)}$ and the normalization, I_B , for the Boson $g_B(r)$'s as a function of density for both the BBGKY-KSA and HNC data where we have defined,

$$I_B = \rho^* \int [g_B(r^*) - 1] d\vec{r}^*. \quad (4.16)$$

In Tables XIII and XIV we list I_B , $\rho_F^{(2)}$, and $\rho_F^{(3)}$ as a function of D for the BBGKY-KSA and HNC $g(r)$'s. Figure 11 shows that in the range of ${}^3\text{He}$ densities Eq. (4.15) is very nearly satisfied by the first two terms in the series. Also there seems to be a definite correlation between I_B and the ratio $\rho_F^{(3)}/\rho_F^{(2)}$ (this is especially evident in Tables XIII and XIV). Naturally, simply because $\rho_F^{(2)}$ and $\rho_F^{(3)}$ alone seem to satisfy Eq. (4.15), does not ensure that $\rho_F^{(4)}$ will be small [for example, Eq. (4.15) could be an alternating series].

TABLE XII. ${}^3\text{He}$ cluster terms resolved into kinetic-energy and potential-energy components for the HNC data. Thus, $E_\alpha = \epsilon_{\text{KE}}^{(\alpha)} + \epsilon_b^{(\alpha)} + \epsilon_{12}^{(\alpha)}$, $\alpha = 1, 2, 3$.

ρ^*	$\epsilon_{\text{KE}}^{(1)}$	$\epsilon_{\text{KE}}^{(2)}$	$\epsilon_{\text{KE}}^{(3)}$	$\epsilon_b^{(1)}$	$\epsilon_b^{(2)}$	$\epsilon_b^{(3)}$	$\epsilon_{12}^{(1)}$	$\epsilon_{12}^{(2)}$	$\epsilon_{12}^{(3)}$
0.15	0.628	-0.108	0.022	-1.156	0.199	-0.063	0.499	-0.137	0.029
0.17	0.730	-0.122	0.026	-1.352	0.217	-0.072	0.595	-0.155	0.034
0.19	0.838	-0.135	0.030	-1.559	0.235	-0.080	0.700	-0.173	0.039
0.21	0.953	-0.149	0.034	-1.776	0.252	-0.089	0.814	-0.192	0.044
0.23	1.075	-0.163	0.038	-2.004	0.269	-0.098	0.940	-0.212	0.049
0.25	1.204	-0.177	0.043	-2.243	0.286	-0.108	1.076	-0.233	0.054
0.27	1.341	-0.191	0.048	-2.493	0.303	-0.117	1.225	-0.254	0.060
0.29	1.486	-0.205	0.053	-2.754	0.320	-0.126	1.387	-0.277	0.066

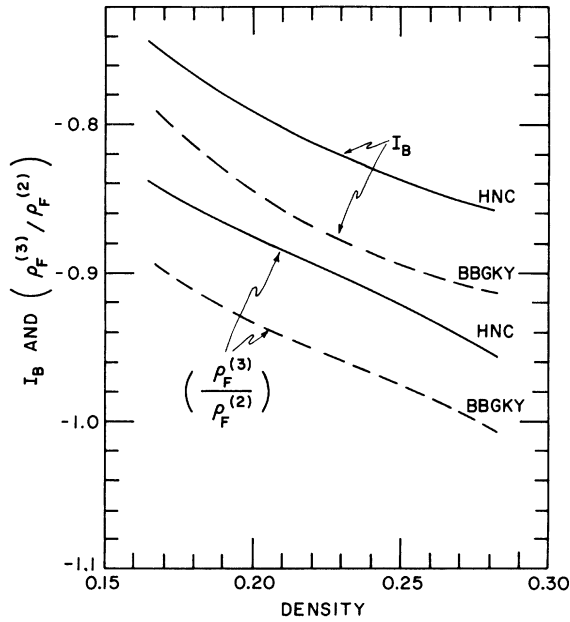


FIG. 11. Ratio of the three-body to two-body statistical cluster corrections for the fermion number density and I_B , the normalization of the boson $g_B(r)$'s for the BBGKY-KSA and HNC data.

V. DISCUSSION

The KSA is clearly a poor approximation to MD at ${}^4\text{He}$ densities. The BBGKY-KSA density at zero pressure, ρ_F^* , is 30% higher than MD while the energy is 15% lower. In fact, the BBGKY-KSA passes below the experimental ${}^4\text{He}$ energies before reaching zero pressure.

Massey and Woo¹⁹ have reported a solution of the BBGKY-KSA equation for ${}^4\text{He}$ with the potential of Eqs. (2.2) and (2.3). Massey and Woo chose, however, to parametrize $g(r)$, rather than $u(r)$, and use the BBGKY-KSA to obtain $u(r)$. Their results are in far better agreement with MD than ours. For example, at zero pressure, their energy is -0.593ϵ at a density of $0.383/\sigma^3 \text{ \AA}^{-3}$. The important difference in variational techniques makes a quantitative comparison between Massey and Woo's and the present results impossible. It is interesting to note, however, that the Massey-Woo $u(r)$ rises much faster than the $u(r)$ of Eq. (2.7) which probably accounts for the good agreement between their $g(r)$'s and those of MD. In that respect it would be interesting to know what MD energies the Massey-Woo wave functions would generate.

Using a result of Abe²⁰ it is possible to make systematic corrections to the KSA. Namely, for a wave function which is a product of pair functions, Abe showed how the three-particle distribution function, $g^{(3)}(r_{12}, r_{23}, r_{31})$, can be written ex-

TABLE XIII. Normalization integral and the cluster corrections to the fermion number density as defined in Eqs. (4.14) and (4.16) for the BBGKY-KSA $g(r)$'s.

D	I_B	$\rho_F^{(2)}$	$\rho_F^{(3)}$	$\rho_F^{(3)}/\rho_F^{(2)}$
0.050	-0.338	-0.746	0.292	-0.391
0.100	-0.535	-0.601	0.343	-0.570
0.150	-0.667	-0.559	0.423	-0.757
0.200	-0.757	-0.540	0.465	-0.862
0.225	-0.791	-0.536	0.478	-0.893
0.250	-0.820	-0.534	0.489	-0.915
0.275	-0.844	-0.533	0.497	-0.933
0.300	-0.864	-0.532	0.504	-0.948
0.325	-0.880	-0.530	0.510	-0.962
0.350	-0.894	-0.528	0.515	-0.976
0.375	-0.905	-0.525	0.521	-0.991
0.400	-0.914	-0.521	0.525	-1.007
0.425	-0.921	-0.517	0.530	-1.024
0.450	-0.926	-0.512	0.534	-1.043
0.475	-0.931	-0.507	0.539	-1.062
0.500	-0.935	-0.502	0.543	-1.081
0.550	-0.942	-0.490	0.550	-1.121
0.600	-0.948	-0.480	0.557	-1.160
0.625	-0.952	-0.475	0.560	-1.178
0.650	-0.957	-0.470	0.562	-1.195
0.675	-0.962	-0.466	0.564	-1.211
0.700	-0.968	-0.461	0.566	-1.226
0.725	-0.975	-0.458	0.567	-1.239
0.750	-0.982	-0.454	0.568	-1.250
0.775	-0.990	-0.451	0.568	-1.261
0.800	-0.999	-0.447	0.569	-1.270
0.850	-1.020	-0.442	0.567	-1.284
0.900	-1.042	-0.436	0.564	-1.293
0.950	-1.067	-0.431	0.560	-1.298
1.000	-1.092	-0.426	0.554	-1.300
1.050	-1.117	-0.420	0.547	-1.301
1.100	-1.142	-0.414	0.539	-1.301

actly in terms of the radial distribution function:

$$g^{(3)}(r_{12}, r_{23}, r_{31}) = g(r_{12})g(r_{23})g(r_{31}) \times \exp\left(\sum_{m=1}^{\infty} \rho^m \delta_{m+3}(r_{12}, r_{23}, r_{31})\right), \quad (5.1)$$

where the δ_{m+3} are cluster integrals. For example,

$$\delta_4 = \int h(r_{14})h(r_{24})h(r_{34}) d\vec{r}_4, \quad (5.2)$$

where $h(r) = g(r) - 1$. In a "perturbative" sense, Sim and Woo²¹ calculated the effect of δ_4 on the KSA energy. They used a solution of the BBGKY-KSA to calculate a small change in $g(r)$ due to the inclusion of the $\delta_4(r_{12}, r_{23}, r_{31})$ term in the BBGKY equation. They found that this raises the energy by approximately 10% which is the right direction to bring the BBGKY-KSA results into agreement with MD. Neither the density dependence of the δ_4 correction nor the importance of higher terms

TABLE XIV. Normalization integral and the cluster corrections to the fermion number density as defined in Eqs. (4.14) and (4.16) for the HNC $g(r)$'s.

D	I_B	$\rho_F^{(2)}$	$\rho_F^{(3)}$	$\rho_F^{(3)}/\rho_F^{(2)}$
0.050	-0.326	-0.622	0.184	-0.296
0.075	-0.433	-0.625	0.271	-0.433
0.100	-0.516	-0.604	0.333	-0.551
0.125	-0.581	-0.581	0.376	-0.647
0.150	-0.634	-0.564	0.406	-0.720
0.175	-0.677	-0.554	0.428	-0.773
0.200	-0.713	-0.548	0.444	-0.810
0.225	-0.743	-0.545	0.456	-0.837
0.250	-0.767	-0.544	0.466	-0.857
0.275	-0.788	-0.544	0.476	-0.873
0.300	-0.806	-0.545	0.484	-0.888
0.325	-0.821	-0.544	0.492	-0.903
0.350	-0.834	-0.544	0.500	-0.919
0.375	-0.846	-0.542	0.508	-0.936
0.400	-0.857	-0.540	0.515	-0.954
0.425	-0.866	-0.537	0.522	-0.972
0.450	-0.875	-0.533	0.529	-0.991
0.475	-0.884	-0.529	0.535	-1.010
0.500	-0.892	-0.525	0.540	-1.028
0.525	-0.900	-0.521	0.545	-1.045
0.550	-0.907	-0.517	0.549	-1.061
0.582	-0.916	-0.512	0.553	-1.079
0.600	-0.920	-0.509	0.555	-1.088
0.625	-0.926	-0.506	0.556	-1.099
0.650	-0.931	-0.503	0.557	-1.107
0.675	-0.936	-0.500	0.557	-1.113
0.700	-0.940	-0.497	0.556	-1.117
0.725	-0.943	-0.495	0.555	-1.120
0.750	-0.946	-0.493	0.553	-1.120

in the series is known.

The fundamental problem of too much correlation in the KSA has been seen in the classical Lennard-Jones system by Broyles, Chung, and Sahlin.²² There are at least two systems, however, for which the BBGKY-KSA has given acceptable results. These are two-dimensional²³ ^4He and the purely repulsive "homework" potential.²⁴ The agreement achieved between the BBGKY-KSA and MD in two-dimensional ^4He is due to the relatively small equilibrium density. As the density is raised, the disagreements become more pronounced and the results resemble those in the bulk.²⁵ In a system with a purely repulsive interaction, like the "homework" neutron matter problem, the particles will try to *maximize* their relative interparticle spacings and thus "overcorrelating" might not be an important fault.

In Appendix C we consider the effect of the Chester-Reatto²⁶ pair function with the zero-point phonons on the BBGKY-KSA energies.

At ^3He densities the BBGKY-KSA appears to be an acceptable approximation to MD. The effective repulsion due to antisymmetry may help mask the

KSA overcorrelation and thus statistics could be a factor which would increase the agreement with MD. It would be interesting to see if the disagreement between MD and BBGKY-KSA is as manifest for " ^4He fermions" as it is for bosons.

As discussed in Sec. IV, at ρ_0^* , E_1 and E_3 are approximately the same size and E_2 contributes 80% of the ground-state energy. There is no numerical problem raised by this large E_2 since it is calculated without approximation. The problem appears in the enhanced role being played by E_3 and the specter of thereby needing some estimate for $E_4 \cdot E_3$ is calculated with both the KSA and convolution approximation (CA) for $g^{(3)}$. There is very little known about the error introduced by the CA in a calculation such as this. However, the use of the CA was confined to the E_{3F} term which itself is only a small part of the three-body contribution to the kinetic energy, for example, using the HNC data at $\rho^* = 0.2$, $E_{3F} \approx -0.006$, out of *total* three-body kinetic energy, $\epsilon_{KE}^{(3)}$, of 0.034. Thus, the major error in E_3 is due to the KSA. We can obtain a crude estimate of this error by comparing our BBGKY-KSA energy with the MD energy for the mass-three boson system. At a density of $\rho^* = 0.237$, SV find $E^* = -0.286$, whereas the BBGKY-KSA yields $E^* = -0.310$, an error of about 10%. It is clear from Fig. 10 that changes in E_3 of this order of magnitude will make very little difference in the relative size of E_2 to E_3 . This is a good sign in so far as the question of rapid convergence of the cluster expansion is concerned; however, it is clear that some reliable estimate of E_4 will have to be made before anything more definite can be stated.

The fundamental difficulty with the statistical cluster series is that with no naturally appearing expansion parameter it is difficult to choose among any reasonable schemes for ordering the terms of the series.

ACKNOWLEDGMENTS

The author would like to express his gratitude to Professor C.-W. Woo who introduced him to the problem and supplied the original BBGKY computer program, to Professor L. H. Nosanow for enlightening discussions on the ordering of the statistical cluster expansion, and to Professor W. J. Mullin for a critical reading of the manuscript. We would like to thank the Department of Physics and Astronomy of the University of Maryland for its hospitality and computer support during the year we were a visitor. The author would also like to acknowledge the computer support from the Vogelback Computer Center of Northwestern University, the Northeast Regional Data

Center of the University of Florida, and the University Computing Center of the University of Massachusetts.

APPENDIX A

In this appendix we shall discuss the numerical solutions of the BBGKY-KSA and HNC integral

$$\theta_{\text{BBGKY}}(R) = -\frac{\pi D}{R} \int_0^\infty u'(S) g(S) \{ (S^2 - R^2) [W_1(R+S) - W_1(R-S)] + 2R [W_2(R+S) - W_2(R-S)] - [W_3(R+S) - W_3(R-S)] \} dS, \quad (\text{A2})$$

and for the HNC equation

$$\theta_{\text{HNC}}(R) = \frac{2\pi D}{R} \int_0^\infty SC(S) [W_1(R+S) - W_1(R-S)] dS \quad (\text{A3})$$

and we have defined

$$W_\alpha(x) = \int_0^x [g(|Y|) - 1] Y^\alpha dy. \quad (\text{A4})$$

The direct correlation function in Eq. (A3) is given by

$$C(S) = g(S) - 1 - \ln [g(S)/e^{u(S)}]. \quad (\text{A5})$$

We note that the functions $W_\alpha(x)$ can be calculated consecutively with the integrations over S and thus both integral equations are *numerically* onefold. The derivation of the form Eq. (A2) for the BBGKY-KSA equation can be found in Hill¹⁰ and has previously been used by Broyles²⁷ to investigate the classical Lennard-Jones (6-12) system. A straightforward derivation of the HNC equation using functional techniques can be found in Ref. 28.

It was convenient to solve the HNC equation in r space rather than the usual momentum representation because this form emphasizes $g(R)$ and avoids the question of the small- k behavior of $S(k)$.

The solutions of Eq. (A1) were obtained by iteration for which the iterative scheme of²⁹ Ng was found to be more convenient and efficient than the usual method of linear combinations of input and output.²⁷ Briefly stated, Ng noted that for the case of *linear* operators one could determine the optimum linear combination of outputs from previous iterations to form a guess for the input to the next iteration. The BBGKY-KSA and HNC equations are certainly *nonlinear*; however, if the input guess is not too far from the solution, the integral equations seem to act like *some* linear operator (over a small set of iterations). For the details of the procedure see the paper by Ng, Ref. 29.

For $D \leq 0.20$ we used $e^{u(R)}$ as the initial guess

equations.

Both equations were solved iteratively in the form:

$$g(R) = e^{u(R) + \theta(R)}, \quad (\text{A1})$$

where for the BBGKY-KSA equation

for both HNC and BBGKY-KSA equations and obtained convergence to (rms) one part in 10^9 in from 8 to 12 iterations. From this point on we proceeded in steps of 0.10 in D using the solution at one step as the initial guess for the next step. For $D \geq 0.60$ we had to decrease the step size to 0.05. We found that an iteration of the HNC equation takes approximately $\frac{2}{3}$ the time of an iteration of the BBGKY-KSA.

APPENDIX B

In Sec. IV we considered the fermion radial-distribution function in the form:

$$g_F(r) = g_B(r) + \Sigma(r) \quad (\text{B1})$$

and we showed that

$$\int \Sigma(r) dr = 0, \quad (\text{B2})$$

because the number density is independent of statistics. One way to interpret Eq. (B2) is to say that the normalization of $g_F(r)$ is completely determined by $g_B(r)$. It is natural to ask how truncating the cluster series affects this relationship. Feenberg considered this question³⁰ and following him we introduce the generalized normalization integral, $\omega(\beta)$, where

$$\omega(\beta) = \left\langle \prod_{i < j} e^{\beta K(r_{ij})} \right\rangle. \quad (\text{B3})$$

In Eq. (B3) the angular brackets are an N -body expectation value and $K(r)$ is an arbitrary function. $\omega(\beta)$ has the property that

$$\frac{d}{d\beta} [\ln \omega(\beta)]_{\beta=0} = \left\langle \sum_{i < j} K(r_{ij}) \right\rangle = N \frac{\rho}{2} \int g_F(r) K(r) d\vec{r}. \quad (\text{B4})$$

Now let us develop Eq. (B4) in a Van Kampen cluster expansion:

$$\frac{d}{d\beta} [\ln \omega(\beta)] = \sum_{m < n} \frac{\omega'_{mn}}{\omega_{mn}} + \sum_{m < n < p} \frac{\omega'_{mnp}}{\omega_{mnp}} + \dots, \quad (\text{B5})$$

where the $\omega_{mn\dots}$ are the usual multiplicative approximants and the primes denote derivatives with respect to β . Examining the three-body term in detail, where we have set the arbitrary function $K(r)$ equal to unity:

$$\frac{\omega'_{mnp}}{\omega_{mnp}} = \frac{\langle (1+1+1)e^{\beta_1} e^{\beta_1} e^{\beta_1} \rangle}{\langle e^{\beta_1} e^{\beta_1} e^{\beta_1} \rangle} - 3 \frac{\langle (1)e^{\beta_1} \rangle}{\langle e^{\beta_1} \rangle}. \quad (\text{B6})$$

We see that the exponentials in Eq. (B6) can be factored out of the expectation values, since they are now constants, to yield

$$\omega'_{mnp}/\omega_{mnp} = 3 - 3 = 0. \quad (\text{B7})$$

Feenberg notes that by definition of the $\omega_{mnp\dots}$ every term in Eq. (B5) of third order and higher will vanish identically in the manner of Eq. (B7). In terms of Eq. (B2) this result can be written

$$\int \Sigma^{(\alpha)}(\vec{r}) d\vec{r} = 0 \quad \text{for } \alpha = 2, 3, \dots \quad (\text{B8})$$

There is an apparent contradiction between Eq. (B8) and the results for the $\rho_F^{(\alpha)}$ [Eq. (4.13)] reported in Tables XIII and XIV which are certainly nonzero. The problem is resolved by noting that the $\Sigma^{(\alpha)}$ in Eq. (4.13) have been obtained after the $\omega_{mn\dots}$ denominators of Eq. (B5) have been expanded in powers of $1/N$. Thus, Feenberg's result is violated to $O(1/N)$. One way to see this is to note that the $\rho_F^{(\alpha)}$ are $O(1)$, whereas the integral of $g(r)$ over all \vec{r} is $O(N)$. Another more interesting way to understand this is to note that Feenberg's result is true for bosons as well as fermions since it only depends on the general form of the multiplicative approximant.

In lowest order of cluster expansion we have for the boson radial-distribution function

$$g_B(r) = \frac{f^2(r)}{[\rho/(N-1)] \int f^2(r) d\vec{r}}, \quad (\text{B9})$$

where $f^2(r) = e^{u(r)}$. The denominator of Eq. (B9) is $1 + O(1/N)$ and is usually simply replaced by 1. If this is done, the integrals over the left- and right-hand sides of Eq. (B9) will differ by a factor of relative $O(1/N)$. If the denominator is kept intact, then the integral over the left-hand side is equal

TABLE XV. Effect of including zero-point phonons in the wave function on the BBGKY-KSA energies at $\rho^* = 0.3648$.

λ (\AA)	$E(\infty) - E(\lambda)$ ($^\circ\text{K}$)
100	0.0
50	-0.0005
20	-0.0012
15	-0.0015
10	-0.0012
8	-0.0002
7	-0.0001
6	+0.0010
5	0.0036
4	0.0049

to the integral over the right-hand side as demanded by Feenberg's theorem.

The $\rho_F^{(\alpha)}$ of Eq. (4.15) have been previously used by Woo¹⁴ to examine the ordering scheme of the cluster expansion.

APPENDIX C

In this appendix we report the effects of including zero-point phonons in the wave function, in the manner of Francis, Chester, and Reatto,³¹ on the BBGKY-KSA energy. The Chester-Reatto long-range wave function is given by

$$u_{\text{LR}}(r) = -(\mu c / \pi^2 \rho^*) [1 / (r^2 + \lambda^2)], \quad (\text{C1})$$

where λ is a momentum cutoff left arbitrary in the theory. Francis, Chester, and Reatto calculated the energy for ^4He using the composite wave function $u_{\text{SR}} + u_{\text{LR}}$ [where u_{SR} , the short-range part, is given by Eq. (2.7)] and treated λ as a variational parameter. We have repeated their calculation using the BBGKY-KSA equation, at the ^4He experimental density $0.3648/\sigma^3 \text{\AA}^{-3}$. We held constant the optimum b (for $\lambda = \infty$) and then varied λ to obtain the results shown in Table XV. The data indicate a possible weak minimum in the energy at about $\lambda = 15 \text{\AA}$ and a definite rise in the energy for small λ . Francis, Chester, and Reatto found an 0.5°K decrease in the energy with $\lambda = 2 \text{\AA}$ using their PY2XS integral equation.

*Work partially supported by a grant from the National Science Foundation.

†Present address: Dept. of Physics and Astronomy, Univ. of Massachusetts, Amherst, Mass. 01002.

¹W. L. McMillan, Phys. Rev. **138**, A442 (1965).

²D. Schiff and L. Verlet, Phys. Rev. **160**, 208 (1967).

³R. D. Murphy and R. O. Watts, J. Low Temp. Phys. **2**, 507 (1970).

⁴C. E. Campbell and E. Feenberg, Phys. Rev. **188**, 396 (1969).

⁵J. C. Lee and A. A. Broyles, Phys. Rev. Lett. **17**, 424 (1966).

- ⁶M. A. Pokrant, *Phys. Rev. A* **6**, 1588 (1972).
- ⁷E. Feenberg, *Theory of Quantum Fluids* (Academic, New York, 1969), p. 218.
- ⁸F. Iwamoto and M. Yamada, *Progr. Theor. Phys. (Kyoto)* **17**, 543 (1957).
- ⁹F. Y. Wu and E. Feenberg, *Phys. Rev.* **128**, 943 (1962).
- ¹⁰For the derivation of the BBGKY equation and its application to the classical liquid see, for example, T. L. Hill [*Statistical Mechanics* (McGraw-Hill, New York, 1956), Chap. 6]; J. M. H. Levelt and E. G. D. Cohen [in *Studies in Statistical Mechanics*, edited by J. de Boer and G. E. Uhlenbeck (North-Holland, Amsterdam, 1964), Chap. 3].
- ¹¹J. G. Kirkwood and E. M. Boggs, *J. Chem. Phys.* **10**, 144 (1942).
- ¹²For a derivation of the virial theorem see Ref. 7, p. 135.
- ¹³These results can be extended to include the wave functions used by J. P. Hansen and D. Levesque [*Phys. Rev.* **165**, 293 (1968)] and J. P. Hansen and E. L. Pollack [*Phys. Rev. A* **5**, 2651 (1972)] to describe the solid helium ground state. Thus, it appears that one should prefer the virial theorem pressures, published by the above authors, over the pressures which they calculated by numerical differentiation. These various wave functions yield results consistent with the virial theorem because the expectation values can be written *explicitly* independent of b , the variational parameter.
- Then b just serves to scale lengths.
- ¹⁴C.-W. Woo, *Phys. Rev.* **151**, 138 (1966).
- ¹⁵S. S. Kuo, *Computer Applications of Numerical Methods* (Addison-Wesley, Reading, Mass., 1972).
- ¹⁶C. Boghosian and H. Meyer, *Phys. Rev.* **152**, 200 (1966); *ibid.* **163**, 206 (1967).
- ¹⁷J. C. Wheatley, *Rev. Mod. Phys.* **47**, 415 (1975).
- ¹⁸Ref. 7, p. 3.
- ¹⁹W. E. Massey and C.-W. Woo, *Phys. Rev.* **164**, 256 (1967).
- ²⁰R. Abe, *Progr. Theor. Phys. (Kyoto)* **21**, 421 (1959).
- ²¹H.-K. Sim and C.-W. Woo, *Phys. Rev.* **185**, 401 (1969).
- ²²A. A. Broyles, S. U. Chung, and H. L. Sahlín, *J. Chem. Phys.* **37**, 2462 (1962).
- ²³M. D. Miller, C.-W. Woo, and C. E. Campbell, *Phys. Rev. A* **6**, 1942 (1972).
- ²⁴S. Chakravarty, M. D. Miller, and C.-W. Woo, *Nucl. Phys. A* **220**, 233 (1974).
- ²⁵C. E. Cambell, M. D. Miller, and C.-W. Woo (unpublished results).
- ²⁶G. V. Chester and L. Reatto, *Phys. Lett.* **22**, 276 (1966).
- ²⁷A. A. Broyles, *J. Chem. Phys.* **33**, 456 (1960).
- ²⁸J. K. Percus, *Phys. Rev. Lett.* **8**, 462 (1962).
- ²⁹K.-C. Ng, *J. Chem. Phys.* **61**, 2680 (1974).
- ³⁰Ref. 7, p. 179.
- ³¹W. P. Francis, G. V. Chester, and L. Reatto, *Phys. Rev. A* **1**, 86 (1970).